ELSEVIER

Biochimica et Biophysica Acta 1466 (2000) 87–104

BIOCHIMICA ET BIOPHYSICA ACTA
BBA

www.elsevier.com/locate/bba

Molecular dynamics study on lipid A from *Escherichia coli*: insights into its mechanism of biological action

Vladimir Frecer [a], Bow Ho [b], Jeak Ling Ding [a,*]

[a] *Department of Biological Sciences, Faculty of Science, National University of Singapore, Science Drive 4, Singapore 117543, Singapore*
[b] *Department of Microbiology, Faculty of Science, National University of Singapore, Science Drive 4, Singapore 117543, Singapore*

Received 6 October 1999; received in revised form 4 January 2000; accepted 21 February 2000

Abstract

Structural properties of the *Escherichia coli* lipid A moiety were analysed by means of molecular mechanics and molecular dynamics simulations and compared to synthetic monophospho and dephospho analogues with different biological activities in the *Limulus* assay. The conformation of glucosamine disaccharide headgroup, order and packing of fatty acid chains, solvation of phosphate groups, coordination by water molecules, sodium counterions and models of cationic amino acid side chains were described in terms of mean values, mean residence times, radial distribution functions, coordination numbers, solvation and interaction energies. Solvation and polar interactions of the phosphate groups were correlated to known biological activities the lipid A variants. The observed relationship between the biological effect and the number and position of the phosphate groups were explained with the help of simple mechanistic models of lipid A action. The possible mechanism of action involving specific binding of lipid A disaccharide headgroup to cationic residues of a receptor model was compared with an alternative mechanism, which assumes a relationship between the ability to adopt non-lamellar supramolecular structures and the biological activity. Conclusions are drawn about the probable mode of lipid A action. Implications for rational drug design of endotoxin-neutralising agents are discussed.

Keywords: Lipopolysaccharide; Lipid A; Conformational analysis; Molecular dynamics; Solvation; Mechanism of action

1. Introduction

Lipopolysaccharides (LPS, also known as endotoxin) represent the major structural components of the outer membrane of Gram-negative bacteria and are responsible for a variety of pathophysiological activities in mammals [1,2]. Stimulation of the host immune system by LPS after bacterial infection leads to physiological events resulting in toxic shock syndromes [3]. LPS is known to form supramolecular aggregates in aqueous solutions that may be implicated in its biological activity [4]. However, in the *Limulus* amebocyte lysate test [5], the LPS monomer

Abbreviations: CD14, cell surface receptor of LPS; GlcN, glucosamine; HDM, 1,16-hexadecanediamine; LA-15-PP, natural lipid A from *Escherichia coli* (1,4′-bisphosphorylated β-(1,6)-linked D-glucosamine disaccharide with six amide-/ester-linked (*R*)-3-hydroxymyristic acid chains; LA-15-HP, synthetic lipid A analogue missing C4′-phosphate group; LA-15-PH, synthetic lipid A analogue missing C1-phosphate group; LA-15-HH, synthetic lipid A analogue missing both C1- and C4′-phosphate groups; LBP, LPS binding protein; LPS, lipopolysaccharide; ReLPS, lipid A and conserved core portion of LPS; TLR, toll-like receptor

* Corresponding author. Fax: +65-779-2486;
E-mail: dbsdjl@nus.edu.sg

0005-2736/00/$ – see front matter
PII: S0005-2736(00)00174-7

[6] has been demonstrated to be more active than the aggregates [7]. Lipid A, the membrane anchor of LPS, is the biologically potent component of LPS [8]. Interactions of lipid A with the surface of target cells are still not fully understood. Non-specific intercalation of lipid A into the phospholipid membrane of the host cell has been considered as a possible mechanism of action [4]. Recently, another mechanism controlling the innate immune responses to LPS challenge has been suggested [9,10]. It assumes lipid A binding to soluble LPS-binding protein (LBP) [11]. The LBP subsequently facilitates transfer of LPS to the cell surface receptor of LPS (CD14) [12], a receptor that participates in LPS-induced cell activation. Most recently some members of the family of human toll-like receptors (TLR2, TLR4) [13,14] have been linked to the LBP/CD14 mediated LPS transmembrane signalling from the host cell surface to the nucleus.

The lipid A of *Escherichia coli* is a 1,4′-bisphosphorylated (1,6)-linked β-D-glucosamine disaccharide with four amide-/ester-linked (*R*)-3-hydroxymyristic acid chains in 2,2′,3,3′ positions of the glucosamine (GlcN) headgroup [15] (Fig. 1). The hydroxy acid chains in 2′,3′ positions are acylated with dodecanoic and tetradecanoic acids, respectively. Bioactivity testing of lipid A variants from different bacterial strains [16] and synthetic lipid A analogues [17] provided some information on the structural requirements determining the endotoxic activity. The three-dimensional structure of LPS receptors and the mode of lipid A binding to these macromolecules remains unknown. Elucidation of the molecular basis for the structure–activity relationships and rationalisation of experimentally observed endotoxic activities of lipid A analogues is therefore much desired. Identification of the molecular mechanism of lipid A binding to the receptors of mammalian cells could namely lead to rational strategies for design of anti-endotoxin therapeutics for treatment of bacterial infections.

Recently, the disaccharide headgroup of lipid A was shown to be essential for binding to the host cells, whereas the hydrophobic fatty acid chains were found to be critical for induction of cytokines [18]. The prominent role of the charged phosphates has been recognised [17,19]. For example, the bioactivities of bisphospho, C1-/C4′-monophospho and dephospho variants of lipid A from *E. coli* span

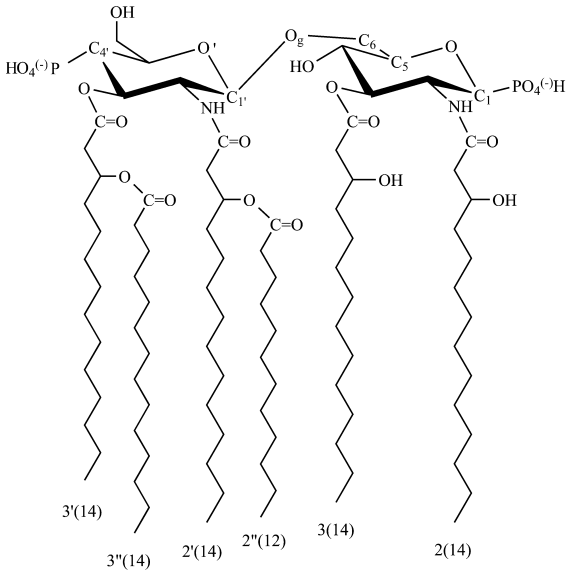

LA-15-PP

Fig. 1. The chemical structure of lipid A from *E. coli*. It consists of 1,4′-bisphosphorylated β-(1,6)-linked D-GlcN disaccharide (GlcN-II-GlcN-I) with four 2,2′-amide- and 3,3′-ester-linked (*R*)-3-hydroxymyristic acid chains. Hydroxyl groups of (*R*)-3-hydroxymyristic chains in 2′,3′ positions are acylated by side chains of dodecanoic (2″) and tetradecanoic (3″) acids. The torsion angles describing the GlcN disaccharide inter-glycosidic linkages are defined as: $\rho=(O',C_{1'},O_g,C_6)$, $\psi=(C_{1'},O_g,C_6,C_5)$ and $\phi=(O_g,C_6,C_5,O)$.

four orders of magnitude in the *Limulus* assay ranging from highly-toxic to non-toxic [17]. Interest in the phosphates was also stimulated by the observation that putative binding sites in LPS-binding proteins [20–22] and endotoxin neutralising antibacterial peptides [23–26] contain higher number of cationic amino acid residues.

In the absence of structural information on the lipid A receptors, the mode of lipid A-receptor binding can be deduced from the structure, symmetry and reactivity of the lipid A variants when correlated with their experimental endotoxic activities. Molecular modelling techniques [27,28] offer the advantage of description of lipid A-receptor interactions at the atomic level when experimental data are missing. Only a limited number of molecular modelling studies have so far been devoted to LPS. Kastowsky et al. [29,30] used molecular modelling to study the three-dimensional structure and conformational flexibility of *E. coli* LPS. Wang and Hollingsworth [31]

studied the structure of *E. coli* lipid A moiety and symmetry patterns in lipid A molecular aggregates. The aggregation of LPS has also been studied with the help of Monte Carlo methods [32] by adopting a simplified geometric representation of LPS molecules. Monte Carlo simulations with NMR derived restraints have been applied to determination of the structure of the core-lipid A region of *Vibrio cholerae* by Vinogradov et al. [33]. Obst et al. [34] carried out a molecular dynamics (MD) study of hydrated lipid A and conserved core portion of LPS (ReLPS) from *E. coli*. However, only limited effort has been devoted to elucidation of the molecular mechanism of lipid A action at the molecular level or quantitative structure–activity relationships of lipid A variants.

The aim of the present work is to explore conformational and dynamic properties of lipid A from *E. coli* and its synthetic monophospho and dephospho variants in aqueous solution to determine whether the observed endotoxic activity [17] can be attributed to particular structural features of the lipid A moiety. Structural and dynamic characteristics obtained from MD and molecular mechanics (MM) simulations were used for evaluation of conformational stability of the disaccharide headgroup, flexibility and order of the acyl chains and solvation and interaction characteristics of functional groups of lipid A analogues. We have attempted to rationalise the observed dependence of the *Limulus* assay activities on the number and position of the phosphate groups in the lipid A moiety by comparing two simple mechanistic models of lipid A action with the experimental bioactivity data. The first mechanism of action assumes specific interactions of the lipid A headgroup with a protein receptor on the host cell surface. The second mechanism relates the molecular shape of the lipid A moiety or the ability to adopt non-lamellar supermolecular structures to its biological effect [4]. Results of the simulations are discussed from both geometric and energetic points of view and conclusions are drawn about the possible molecular mechanism of lipid A action. Strategies for rational design of anti-endotoxin agents are also proposed.

2. Computational methods

2.1. Lipid A moiety

The crystal structure of LPS attached to the surface of the ferric hydroxamate uptake receptor [35] was used as the starting model of the *E. coli* lipid A moiety (the natural lipid A from *Escherichia coli* (1,4′-bisphosphorylated β-(1,6)-linked D-glucosamine disaccharide with six amide-/ester-linked (*R*)-3-hydroxymyristic acid chains (LA-15-PP)). The general shape of the molecule, mutual orientation of the GlcN rings, conformation of the amide-/ester-linkages and the parallel alignment of the six fatty acid chains in the crystal structure [35] were adopted in the initial model. The starting conformation of β-(1,6)-glycosidic linkage of the disaccharide headgroup (GlcN-II-GlcN-I) was taken from modelling studies in solution [34] and was further explored by a full conformational search. The model of LA-15-PP was refined using the Biopolymer module of the InsightII program, version 97.0 [36] (Fig. 2). The structures of synthetic monophospho and dephospho variants of the lipid A lacking the C1-phosphate group (LA-15-PH), C4′-phosphate group (LA-15-

Table 1
Notation and structure of lipid A from *E. coli* and its synthetic monophospho and dephospho analogues

Analogue[a]	R(4′)[b]	R(3′)	R(2′)	R(3)	R(2)	R(1)
LA-15-PP	PO_4H^-	C_{14}-O-(C_{14})	C_{14}-O-(C_{12})	C_{14}-OH	C_{14}-OH	PO_4H^-
LA-15-PH	PO_4H^-	C_{14}-O-(C_{14})	C_{14}-O-(C_{12})	C_{14}-OH	C_{14}-OH	OH
LA-15-HP	OH	C_{14}-O-(C_{14})	C_{14}-O-(C_{12})	C_{14}-OH	C_{14}-OH	PO_4H^-
LA-15-HH	OH	C_{14}-O-(C_{14})	C_{14}-O-(C_{12})	C_{14}-OH	C_{14}-OH	OH

[a]Notation of the lipid A analogues was taken from [17] and references cited therein.
[b]LA-15-PP, LA-15-PH, LA-15-HP and LA-15-HH analogues denote 1,4′-diphosphate, 4′-monophosphate, 1-monophosphate and dephospho lipid A analogues, respectively; C_{14}-OH – (*R*)-3-hydroxytetradecanoyl; C_{14}-O-(C_{14}) – (*R*)-3-tetradecanoyloxytetradecanoyl; C_{14}-O-(C_{12}) – (*R*)-3-dodecanoyloxytetradecanoyl. The O-(C_{14}) acyl chain branch in position R(3′) is also denoted as C3″-O-acyl chain and the O-(C_{12}) acyl chain branch in position R(2′) is also denoted as C2″-N-acyl chain in the text.

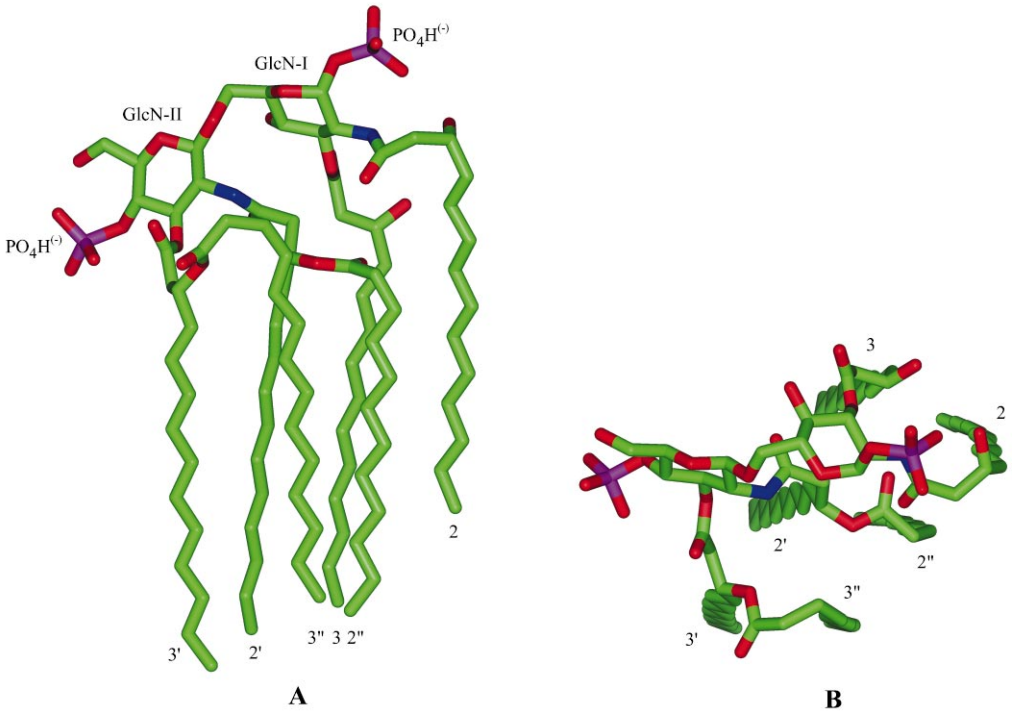

Fig. 2. Stick drawings of the most stable lipid A LA-15-PP *gtggcttc* conformer. (A) Side view and (B) top view show the compact packing of six all-*trans* parallel aligned fatty acid chains linked to the GlcN-II-GlcN-I headgroup. The overall shape of the molecule is cylindrical. Numbering of the fatty acids chains is derived from the attachment atom number of the GlcN ring (2″ and 3″ are the branch chains in 2′,3′ positions). Hydrogen atoms have been omitted for better clarity.

HP) or both (LA-15-HH) [17] were derived from the LA-15-PP model by replacing the individual phosphates with hydroxyl groups (Table 1). A formal charge of -1 *e* was assigned to each phosphate group with a net charge of -0.85 *e* placed on each non-protonated oxygen. All atomic charges were taken from the force field library and were used consistently throughout the study. Sodium counterions were added to neutralise the phosphate groups in solution at physiological conditions. The initial position of the Na^+ ions in the vicinity of the phosphates was refined by minimisation in vacuum. Na^+ ions were assigned a formal charge of +1 *e*.

A 1,16-hexadecanediamine moiety (HDM) with two charged ammonium groups was used as a simple pseudoreceptor model, which represented two cationic amino acid side chains of spatially constrained lysine residues. The HDM was docked to the lipid A analogues in an all-*trans* conformation with the ammonium groups approaching the phosphates. The mutual positions of the PO_4H^- groups of lipid A and NH_3^+ groups of HDM were refined by minimisation in vacuum. The ammonium groups of HDM were assigned a formal charge of +1 *e* with a net charge of 0.28 *e* placed on each hydrogen.

2.2. MM and MD simulations

MM and MD simulations on four solvated lipid A analogues were carried out by the Discover program, version 2.97 [36], using all-atom representation. Class II consistent force field (CFF91) [37,38] was applied throughout the study. This force field uses Morse potential to model covalent bonds, includes an anomeric carbon atom and does not possess explicit hydrogen bonding potential term. CFF91 has been previously used successfully in molecular modelling of carbohydrates [39,40], hydrogen bonding interactions [41] and conformational analyses [42].

To explore the conformational space of β-(1,6)-glycosidic linkages of the lipid A headgroup, all combinations of the torsion angles $\rho = (O', C_{1'}, O_g, C_6)$, $\psi = (C_{1'}, O_g, C_6, C_5)$, $\phi = (O_g, C_6, C_5, O)$ (Fig. 1) were sampled in a complete search for stable lipid A con-

formations. The same starting configuration with compact alignment of fatty acid chains was used for each $\{\rho,\psi,\phi\}$ point of the conformational energy hypersurface for a given lipid A analogue. Only a lipid A conformation with fully aligned acyl chains can act as a hydrophobic membrane anchor of LPS [1], or form supramolecular aggregates in solutions [4]. Therefore, only the configurations with parallel fatty acid chain arrangements were explored. The torsion angles were sampled from −180° to 180° with an increment of 30° using a torsion forcing expansion term with a force constant of 100 kcal mol^{-1} rad^{-2}. Each of the 2197 generated lipid A conformations was extensively minimised using steepest descent and conjugate gradient algorithms until convergence was reached at the gradient of 0.01 kcal $mol^{-1}Å^{-1}$. The dielectric constant was set to one during all MM, MD simulations. Boltzmann probability distributions $P\{\rho,\psi,\phi\}$ [43] were calculated from the relaxed MM potential energy hypersurface $E_{MM}\{\rho,\psi,\phi\}$ for each $\{\rho,\psi,\phi\}$ point. This probability describes the extent of rotational freedom about the glycosidic bonds and the relative populations of individual low-energy conformational states. It is defined as:

$$P\{\rho, \psi, \phi\} = \exp[-E_{MM}\{\rho, \psi, \phi\}/RT]/\Sigma_{\rho,\psi,\phi} \exp[-E_{MM}\{\rho, \psi, \phi\}/RT] \quad (1)$$

where R is the gas constant and T is the temperature. Highly populated conformational states with compact alignment of the acyl chains has been classified according to the conformations of exocyclic side groups of the $^4C_1$ D-GlcN rings GlcN-II and GlcN-I. Hydroxymethyl groups had either *gauche-gauche* (*gg*) or *gauche-trans* (*gt*) orientations (relative to ring C4 and O atoms, respectively) [44]. *Cis* (*c*) and *trans* (*t*) orientations of the NH and O–C=O groups of amide-/ester-linkages (relative to the pertinent ring carbon protons) were found. Notation for the headgroup conformations is given with the following order of the relevant functional groups {C6′,C6,2′,3′,2,3}.

Conformational flexibility of the glycosidic linkages of the GlcN-II-GlcN-I headgroup, amide-/ester-linkages and fatty acid chains of solvated lipid A analogues were studied by MD simulations. The MD simulations were performed in NVT ensemble. Monomers of lipid A analogues were immersed in a rectangular solvent box of the size $(26\times30\times22)$ $Å^3$ filled with approximately 450 pre-equilibrated water molecules at 300 K. The size of the box allowed at least 4 Å distance from the lipid A moiety to the boundaries of the box. Periodic boundary conditions were used in x, y and z directions [45]. The system was heated from 0 to 300 K over a period of 5 ps and allowed to equilibrate for 5 ps. Data collection was carried out for 100 ps, the trajectory was averaged and recorded every 50 steps (over 0.05 ps intervals) and the non-bonded atom list was updated every 10 steps. Standard deviations (S.D.) of dynamic quantities were obtained by averaging over 2000 coordinate sets generated during the data collection period and expressed as the mean ± S.D. MD simulations on solvated lipid A analogues complexed with a single HDM molecule were carried out in the same periodic box including approximately 430 water molecules.

The studied small-amplitude internal motions corresponding to conformational flexibility within the low-energy region of the conformational space include internal motions around the glycosidic linkage, orientation of phosphate and hydroxyl groups, relaxation of the acyl chains, solvent molecules rearrangement and counterion coordination. These motions fluctuate on a fast timescale of vibrational and rotational motions, which have correlation times shorter than the MD simulation time [46–55].

The dimensions of the solvent box permitted full conformational flexibility of the solute. The lipid A analogues in the box were covered by several solvation shells (the minimum number of solvent shells at the point of closest distance to the box boundaries was two). The simulations took into account the main driving forces that affect the structure and dynamics of carbohydrates, namely intra-molecular and solute-solvent hydrogen bonding and van der Waals interactions [49], which mainly involve the solvent molecules of the first few solvation shells [52,53]. In this study we have estimated relative trends in the explicit and implicit solvation energies among various lipid A analogues and simulated the effect of specific solute-solvent interactions upon relative changes in the energies of ion-pair formation of the phosphate groups. For such purposes even the relatively modest number of explicit water molecules (ap-

proximately 450) provides a sufficiently clear picture [52,53].

The conformations of solvated headgroups of lipid A analogues were analysed in terms of averaged glycosidic linkage torsion angles $\{\rho,\psi,\phi\}$ and their mean residence times (MRT). Trajectories from the data collection period were used for calculation of radial pair distribution functions (RDF) of water molecules, sodium ions around the phosphate and hydroxyl groups. Coordination numbers (CN) of the phosphates were also evaluated. RDFs represent the probability of finding the relevant species at a distance of $\langle r, r+dr\rangle$ as a function of the distance r from the central atom during the simulation. They characterise solvation properties and ion-pair formation characteristics of the functional group. CNs were obtained by integration of RDFs and show the number of the particles in each solvation shell. MRTs are particularly useful dynamic characteristics of the solute structure and solvent mobility [56] and represents the portion of the MD simulation time during which a measured quantity acquires particular value. RDF, CN and MRT have been previously used for characterisation of hydration of ReLPS from *E. coli* [34].

2.3. Solvent effects and molecular electrostatic potential (MEP)

MD trajectories of solvated lipid A analogues were used to assess the effect of the solvent in relation to the number and position of phosphate groups in the lipid A moiety. A quantity proportional to the explicit solvation energy (E^{E}_{solv}) was derived by averaging the instant solute-solvent interactions of the lipid A analogues with approximately 450 water molecules in the periodic solvent box over 200 coordinate sets recorded every 0.5 ps during the 100 ps MD simulation trajectory. The E^{E}_{solv} values were corrected for the number of water molecules in the box and compared to solvation energy values of lipid A analogues derived from continuum solvent models. Solvation energy of the lipid A analogue in water represents a quantity that describes the polarity and ionic character of the molecules and is useful for estimation of binding free energies in the condensed phase [57].

The polarisable continuum model (PCM) [58–60] represents the solvent as a homogeneous medium, characterised by macroscopic properties, such as dielectric constant. It employs rigorous treatment of solute–solvent interactions including the electrostatic, dispersion and repulsion terms and involves the cavitation term that accounts for creation of a realistic cavity reproducing van der Waals molecular surface of the solute. The PCM model solves the Laplace equation for the solute charge distribution using the boundary element method [59]. A dielectric constant of 1.0 was used for the solute and 80.0 for water. The atomic radii and charges were taken from the CFF91 force field. The atomic polarisabilities of Thole [61] were used in the dispersion term.

Solvation energies were also calculated using the DelPhi module [36], which solves the Poisson–Boltzmann equation using the finite difference method assuming continuum representation of the solvent. The coordinates of the solvated lipid A analogues were mapped onto a three-dimensional grid with a resolution of 0.20 Å per grid point and a border space of 40% of the grid size. The dielectric constant of the solute and the surrounding water were set to 1.0 and 80.0, respectively. The atomic radii and charges were taken from the CFF91 force field.

The MEP was calculated for the solvated headgroups of lipid A analogues from the Poisson–Boltzmann equation using the DelPhi module. The resulting MEP was mapped onto van der Waals molecular surface of the lipid A headgroups and the contours were coloured according to the MEP magnitudes.

2.4. Order and packing of fatty acid chains

The dynamic behaviour, shape and packing of the six aliphatic fatty acid chains in the lipid A analogues were investigated in terms of order parameter (S_c), packing parameter (P) and average chain length (L_{aver}). The order parameter describes the orientation of methylene groups of the fatty acid chains of lipid A moiety relative to a reference vector. It was calculated from the average angle, θ, between a C–H bond vector of a methylene group in the fatty acid chain and the reference vector, as: $|S_c| = |(3\langle\cos^2\theta\rangle-1)/2|$ [62]. The centre of mass of the lipid A headgroup was connected to the centre of mass of the acyl chain portion of the molecule by

a reference vector [34]. The angle θ has been averaged over the lipid A trajectory and the corresponding $|S_c|$ depicts the dynamic behaviour of the 10 last methylene groups of the six acyl chains {2,3,2′,2″,3′,3″}.

According to the theory of Israelachvili [63], the packing parameter characterises the ability to form supramolecular aggregates by packing of the monomers. Packing of lipid A molecules can be estimated from geometric parameters such as cross-section (a_o) of the hydrophilic headgroup GlcN-II-GlcN-I and the hydrophobic fatty acid chain portion (V/l_c) of a lipid A monomer using the formula: $P = V/(a_o l_c)$. The critical chain length (l_c) and volume of the hydrophobic portion of the moiety (V) can be evaluated by the formulas given by Tanford [64] as: $l_c = (1.54+1.27n)$ Å and $V = (27.40+26.90n)$ Å^3, for a saturated hydrocarbon chain with n carbon atoms. Depending on the packing parameter value, the formation of spherical micelles ($P < 1/3$), globular or cylindrical micelles ($1/3 < P < 1/2$), vesicles ($1/2 < P < 1$), planar bilayers ($P \cong 1$), or inverted micelles ($P > 1$) is predicted. The averaged headgroup cross-section, a_o, of the lipid A analogues was derived from the MD simulation data as a projection of the GlcN-II-GlcN-I headgroup to a plane perpendicular to the reference vector assuming an approximate rhomboid shape of the headgroup projection.

The chain length was calculated by averaging the distance between the ending methyl group and the 12th methylene group from the acyl chain end over the MD trajectory for the solvated lipid A analogues. The L_{aver} was also averaged over the six fatty acid chains {2,3,2′,2″,3′,3″} for each lipid A analogue.

The average tilt angle between the axis of the disaccharide headgroup connecting the centres of mass of GlcN-II and GlcN-I rings and the normal vector in the direction of the fatty acid chains, was computed for each snapshot conformation and averaged over the whole MD trajectory. The average bend angle between two planes intersecting the {O′,C2′,C4′} and {O,C2,C4} atoms of the two rings GlcN-II and GlcN-I was calculated from the MD trajectory. It describes the shape of the disaccharide headgroup and the mutual orientation of the GlcN rings.

3. Results and discussion

3.1. Structure of lipid A molecule

Conformations of β-(1,6) glycosidic linkages in the LA-15-PP, LA-15-PH, LA-15-HP and LA-15-HH analogues (Table 1) were explored by a full conformational search over the torsion angles $\{\rho,\psi,\phi\}$. Only the conformations with compact alignment of the fatty acid chains were considered since these are expected to form the lipid A configuration integrated in the outer layer of bacterial membrane or to be present in polar solvents due to hydrophobic interactions. Table 2 lists the relative energies (ΔE_{rel}), location of the minima on the $E_{MM}\{\rho,\psi,\phi\}$ hypersurface, Boltzmann probabilities of the conformations $P\{\rho,\psi,\phi\}$ and r.m.s. deviations of the GlcN-II and GlcN-I rings of the global minimum conformations of the monophospho and dephospho lipid A analogues from those in the LA-15-PP minimum energy conformation. The global minimum energy conformation of the β-(1,6) glycosidic linkages of all the studied analogues laid in the same region of the potential energy hypersurface, near the point $\{\rho,\psi,\phi\} = \{-87,-103,-66\}°$. A collection of low-energy conformations with Boltzmann population probabilities $P\{\rho,\psi,\phi\}$ between 1 and 5% and relative energy differences $\Delta E_{rel} < 2.5$ kcal mol^{-1} with respect to the global energy minimum were found in the vicinity of the global minimum for each lipid A analogue. In these conformations a minor shift along the ρ, ψ or ϕ directions typically did not exceed 20°. All the low-energy conformations retained the compact parallel alignment of the fatty acid chains and the *cttc* conformation of the {2′,3′,2,3} amide-/ester-linkages present in the starting conformation *gtggcttc* (Fig. 2). In the global minimum structure the hydroxymethyl group of the GlcN-I ring involved in the β-(1,6) linkage acquired the *gg* conformation.

Mutual positions and orientations of the GlcN-II and GlcN-I rings and the phosphate groups were preserved in the global minimum conformations of the lipid A analogues. The positions of the GlcN remained within averaged r.m.s. deviation of 0.12 Å for the heavy atoms compared to the global minimum conformation of LA-15-PP (Table 2). Planes of the two GlcN rings retained an almost constant bend angle of approximately 62° for all lipid A analogues

with relatively low standard deviations, which indicate rigidity of the headgroup configuration. In the global minimum conformation the orientation of the C4′-phosphate group was stabilised by a hydrogen bond to C6′-OH group of the GlcN-II. The C1-phosphate group was linked by hydrogen bonds to C2-NH group, and -OH group of the C2 amide-linked (*R*)-3-hydroxymyristic acid chain.

Low populated alternative *gtgtcttc* conformation with *gt* conformation of the C6 hydroxymethyl group of the GlcN-I ring shared the overall molecular shape, compact alignment of the fatty acid chains and orientation of the GlcN-II and GlcN-I rings with the global minimum conformation of the LA-15-PP. The less stable *gtgtcttc* conformers of the GlcN rings were linked by an inter-residue hydrogen bond C2′–NH···OH–C4. The conformation of the flexible β-(1,6) glycosidic linkages was, however, different. The $\{\rho,\psi,\phi\}$ torsion angles of these conformations were equal to approximately {48,145,170}° (Table 2). The position and orientation of the GlcN-II and GlcN-I rings, however, resembled that of the more stable *gtggcttc* conformation.

Wang and Hollingsworth [26] reported a stable conformation with torsion angles $\{\rho,\psi,\phi\} = \{-75, -97, -53\}°$ for a model of a bisphospho headgroup of lipid A using MM2 and Dreiding force fields, which compares well with our results obtained for the stable *gtggcttc* conformation. Obst et al. [34] found the glycosidic torsion angles averaged over a set of six bisphospho *E. coli* ReLPS conformations $\{\rho,\psi,\phi\} = \{-65, -160, -70\}°$ with closely packed acyl chains in a MD simulations in water using CHARMM force field. The average $\{\rho,\psi,\phi\}$ torsion angles lie in the same energy hypersurface region as our predicted values for the lipid A analogues.

No significant geometrical differences in the molecular shape, mutual position and orientation of the GlcN rings, orientation of the phosphate groups or compact alignment of the fatty acid chains were found for the stable *gtggcttc* conformations of the four considered lipid A analogues. The number and position of the phosphate groups in the chemical structure of the lipid A moieties did not impose significant consequences upon the conformation or intra-molecular interactions of the lipid A analogues that could be directly related to varying experimental biological activities of these molecules.

3.2. MEP of lipid A headgroups

The MEP pattern mapped onto the molecular van der Waals surface illustrates the significance of charged or polar reactive functional groups such as PO_4H^- in the bisphospho, monophospho and dephospho lipid A analogues (Fig. 3). Clear patterns

Table 2
Energy minima and torsion angles of β-(1,6)-glycosidic linkages of lipid A analogues.

Analogue[a]	ΔE^{b}_{rel}	$P\{\rho,\psi,\phi\}$[c]	ρ[d]	ψ	ϕ	r.m.s.d.[e]	Conformation[f]
LA-15-PP	0.0	57.4	−89	−102	−62	0.0	*gtggcttc*
	5.2	0.0	46	142	163	–	*gtgtcttc*
LA-15-PH	0.0	56.3	−87	−105	−68	0.11	*gtggcttc*
	8.8	0.0	47	143	174	–	*gtgtcttc*
LA-15-HP	0.0	53.8	−87	−100	−64	0.04	*gtggcttc*
	3.5	0.0	50	147	174	–	*gtgtcttc*
LA-15-HH	0.0	55.6	−84	−105	−68	0.12	*gtggcttc*
	5.0	0.0	45	150	171	–	*gtgtcttc*

[a]Notation of the lipid A analogues is given in Table 1.

[b]MM energy of a conformer relative to the minimum energy conformation (kcal mol^{-1}).

[c]Boltzmann population probability of *gtggcttc* and *gtgtcttc* conformations (%).

[d]Torsion angles of the β-(1,6)-glycosidic linkages, $\rho = (O',C_{1'},O_g,C_6)$, $\psi = (C_{1'},O_g,C_6,C_5)$, $\phi = (O_g,C_6,C_5,O)$ (Fig. 1).

[e]r.m.s. deviation of heavy atoms in GlcN-II and GlcN-I D-GlcN rings compared to those of the LA-15-PP minimum energy *gtggcttc* conformation (Å).

[f]Conformation of hydroxymethyl groups of GlcN-II and GlcN-I rings: *gg* or *gt* (relative to ring C_4 and O atoms, respectively [44]. *c* and *t* orientations of the NH and O–C=O groups of the amide-/ester-linkages of GlcN-II and GlcN-I rings (relative to the ring carbon protons). Notation of conformations is in the following order {C6′,C6,2′,3′,2,3}. Only the conformations with compact parallel alignment of fatty acid chains were considered.

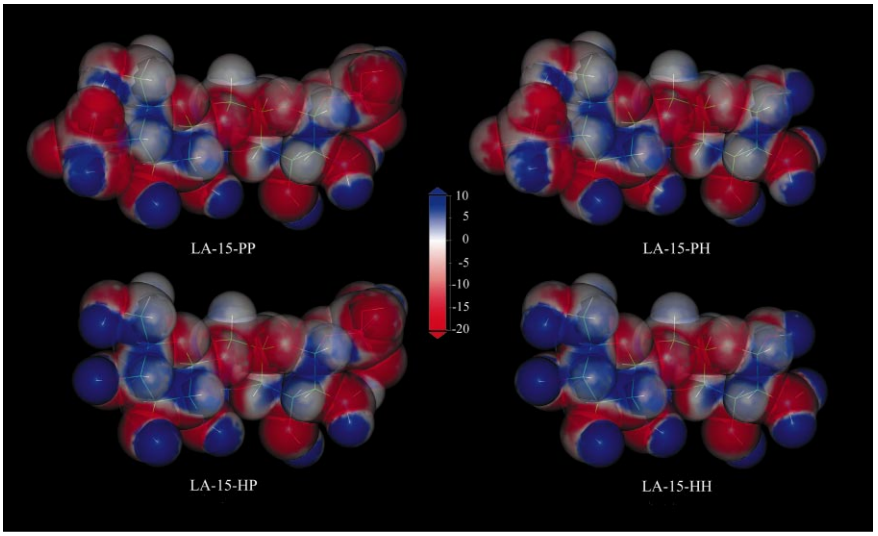

Fig. 3. MEP of solvated headgroups of lipid A analogues. MEP was mapped on the van der Waals molecular surface of the lipid A analogues coloured by a continuous spectrum (red to blue) that corresponds to partially transparent MEP contours ranging from −20 to 10 kcal mol^{-1} e^{-1}.

of negative MEP contours centred on the charged phosphate groups display the tendency of the phosphate groups to engage in electrostatic interaction such as ion-pair formation or hydrogen bonding. Polar amide-/ester groups that link the fatty acid chains to the disaccharide headgroup are sterically less accessible and thus the exocyclic phosphates and the hydroxyl groups represent the most reactive centres in the lipid A molecular structures. It is therefore likely that the observed differences in experimental bioactivity among the bisphospho, monophospho and dephospho analogues (Table 3), which range four orders of magnitude from highly active to non-active substances, are related to the number and position of the phosphate groups in the lipid A moiety.

3.3. Dynamics of lipid A molecules in solution

The stable conformations of the glycosidic linkages of the lipid A analogue headgroups obtained by full conformational search in vacuum were also preserved during the MD simulations in solution. The dynamic and structural properties derived from the MD trajectories of solvated lipid A analogues are summarised in Table 3. The GlcN-II-GlcN-I headgroups of all four analogues exhibited similar conformation of the $\{\rho,\psi,\phi\}$ torsion angles in water. Only minor dependence of the glycosidic linkage conformations on the number and position of the phosphate groups in the lipid A moiety was detected. The ψ torsion angle was more susceptible to variations. The solvated headgroups of all analogues showed only limited flexibility of the glycosidic linkages as expressed by small standard deviations from the mean $\{\rho,\psi,\phi\}$ values (Table 3). The $\{\rho,\psi,\phi\}$ angles of solvated LA-15-PP in the presence of two Na^+ counterions displayed average values of $\{-89,-142,-67\}°$ (Fig. 4A,B). This average conformation resembled that of the hydrated ReLPS from *E. coli* [34] coordinated by two Ca^{2+} ions with the mean torsion angles $\{-75,-161,-76\}°$. The overall shape of each studied lipid A analogue was also retained during the simulation time and no transition between structures distant in the conformational space was observed. The flexibility of the amide-/ester-linkages connecting the acyl chains to the GlcN rings was limited and no change in the starting *cttc* configuration of these linkages occurred during the simulation. This is probably due to the stabilising effect of the solute–solvent non-bonding interactions and damping of high frequency motions of the solute.

Fig. 4C shows an important parameter that may be crucial for the recognition of lipid A by a protein receptor, namely, the average distance between the

Table 3
Structural and dynamic properties of solvated lipid A from *E. coli* and its synthetic analogues

Property	LA-15-HH[a]	LA-15-HP	LA-15-PH	LA-15-PP	LA-15-PP Na
Toxicolor test[b]	0.00113	0.044	0.83	5.52	5.52
Q_{LA} [c]	0	−1	−1	−2	−2
E^{E}_{solv} [d]	−232 ± 41[q]	−347 ± 56	−391 ± 54	−479 ± 61	−572 ± 79[r]
N_{wat} [e]	456	453	451	450	448
E^{D}_{solv} [f]	−57	−108	−124	−215	–
E^{P}_{solv} [g]	−119	−183	−201	−277	–
E^{E}_{int} [h]	−248 ± 14[q]	−393 ± 18	−443 ± 19	−561 ± 24	–
ρ[i]	−85 ± 13[s]	−84 ± 11	−83 ± 11	−83 ± 11	−89 ± 13
ψ	−115 ± 20[s]	−124 ± 17	−131 ± 15	−128 ± 14	−142 ± 17
ϕ	−64 ± 8[s]	−64 ± 8	−73 ± 11	−71 ± 11	−66 ± 10
d(P1–P4′)[j]	10.4 ± 0.2[t,u]	11.6 ± 0.6[t]	11.8 ± 0.4[u]	13.3 ± 0.2	13.1 ± 0.3
G_{aw}(R) P4′[k]	2.9[t]	2.9[t]	3.7	3.8	3.8
N_{aw}(R) P4′	1.7[t]	1.9[t]	4.5	4.7	3.8
G_{aw}(R) P1	2.9[u]	3.7	2.9[t]	3.7	3.8
N_{aw}(R) P1	2.4[u]	4.9	2.4[t]	4.9	4.7
G_{ana}(R) P4′[l]	–	–	–	–	6.5, 8.2[v]
N_{ana}(R) P4′	–	–	–	–	0.2, 0.6[x]
G_{ana}(R) P1	–	–	–	–	7.8
N_{ana}(R) P1	–	–	–	–	0.9
Bend[m]	60 ± 7[s]	62 ± 8	62 ± 7	63 ± 5	63 ± 4
Tilt[n]	84 ± 1[s]	69 ± 13	75 ± 17	87 ± 13	96 ± 13
L_{aver} [o]	12.9 ± 1.0[s]	12.3 ± 1.6	12.1 ± 2.3	12.6 ± 1.4	12.8 ± 1.0
P[p]	1.5	1.1	1.1	0.9	0.9

[a]For notation of lipid A analogues see Table 1. LA-15-PP Na denotes solvated LA-15-PP coordinated by two Na^+ ions.
[b]Biological activity of lipid A analogues, measured by the activation of clotting enzyme cascade in the *Limulus* assay (Toxicolor test [5]) was taken from [17].
[c]Molecular charge of the lipid A analogue (e).
[d]Quantity proportional to solvation energy of lipid A analogues derived from the explicit solvent model (kcal mol^{-1}).
[e]Number of water molecules in the solvent box with dimension $(26\times30\times22)$ $Å^3$.
[f]Solvation energy of lipid A analogues derived from the DelPhi continuum solvent model [36] (kcal mol^{-1}).
[g]Solvation energy of lipid A analogues derived from the PCM continuum solvent model [58–60] (kcal mol^{-1}).
[h]Interaction energy of lipid A analogues with HDM as a simple model for two constrained cationic amino acid residues (Lys) of a receptor binding site, derived from the explicit solvent model (kcal mol^{-1}).
[i]Torsion angles of the inter-glycosidic linkage and C6–C5 bond: ρ=(O′,C1′,Og,C6), ψ=(C1′,Og,C6,C5), ϕ=(Og,C6,C5,O) (Fig. 1) (°), for notations of atoms see Fig. 1.
[j]Interatomic distance between phosphorus atoms of the C1- and C4′-phosphate groups (Å).
[k]Pair radial distribution function G_{aw}(R) and CN N_{aw}(R) of water oxygen atoms around the phosphorus atoms of the C1- and C4′-phosphate groups.
[l]Pair radial distribution function G_{ana}(R) and CN N_{ana}(R) of Na^+ ions around the phosphorus atoms of the C1- and C4′-phosphate groups.
[m]Average bend angle between the GlcN ring planes intersecting the {O′,C2′,C4′} and {O,C2,C4} atoms of the GlcN-II and GlcN-I rings (°).
[n]Average tilt angle between the backbone axis of the GlcN-II-GlcN-I headgroup and vectors aligned along the fatty acid chains averaged over the six {2,3,2′,2″,3′,3″} chains (°).
[o]Average chain length of the fatty acids chains of lipid A, averaged over the six {2,3,2′,2″,3′,3″} chains (Å).
[p]Mean packing parameter $P = Vl/(a_o l_c)$.
[q]S.D. obtained from averaging 200 coordinate sets recorded every 0.5 ps of the 100 ps MD simulation. Values are expressed as average ± S.D.
[r]Solvation energy of LA-15-PP Na includes also the interaction of a lipid A molecule with two Na^+ ions in the E^{E}_{solv} value.
[s]S.D. obtained from averaging 2000 coordinate sets recorded every 0.05 ps of the 100 ps MD simulation. Torsion angle values are expressed as average ± S.D.
[t,u]Computed for C4′-OH or C1-OH groups instead of phosphate groups.
[v]Two distinct peaks were observed on the G_{ana}(R) curve for the C4′-phosphate group.
[x]N_{ana}(R) for the second peak represents its net contribution.

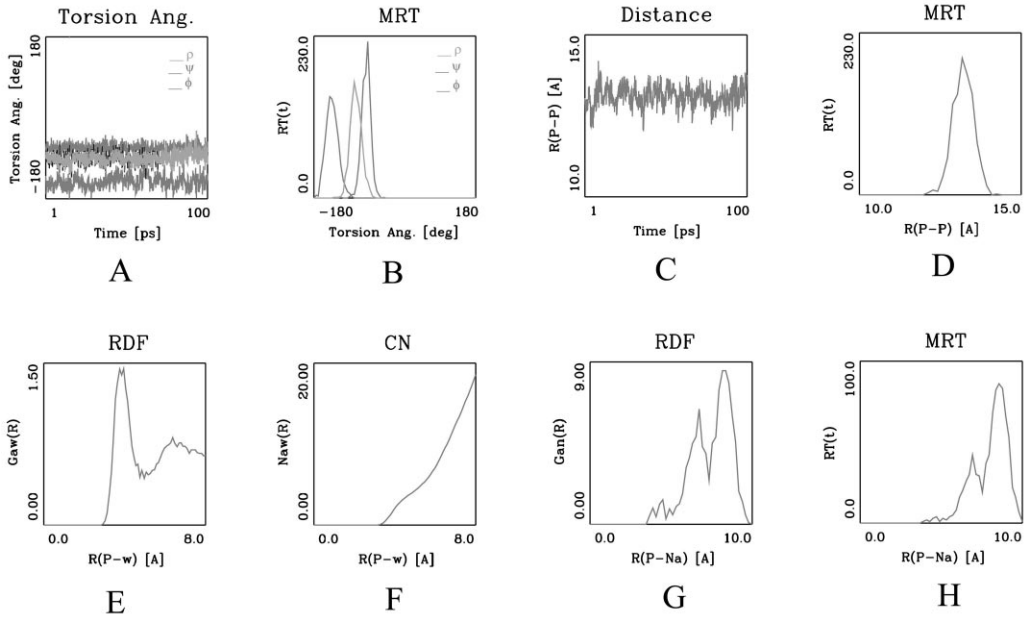

Fig. 4. MD simulation on solvated lipid A from *E. coli* with phosphate groups coordinated by two sodium ions. (A) Time evolution of the β-(1,6)-glycosidic linkages of the GlcN disaccharide of LA-15-PP $\{\rho,\psi,\phi\} = \{-89,-142,-67\}°$. (B) MRT curves of $\{\rho,\psi,\phi\}$ torsion angles averaged over 100 ps MD simulation trajectory. (C) Distance between phosphorus atoms of C1- and C4′-phosphate groups R(P–P) (Å). (D) MRT of R(P–P). (E) Radial distribution function $G_{aw}(R)$ of oxygen atoms of water around the phosphorus of the C4′-phosphate group; (F) CN $N_{aw}(R)$ of oxygen atoms of water around the phosphorus of the C4′-phosphate group derived from the $G_{aw}(R)$ curve; (G) radial distribution function $G_{ana}(R)$ of Na^+ ions around the phosphorus of the C4′-phosphate group; (H) MRT curve of R(P–Na) distance of Na^+ ions surrounding the phosphorus of the C4′-phosphate group.

charged C1- and C4′-phosphate group centres, *d*(P–P). The MRT curve of the *d*(P–P) reached its peak value at the separation of 13.1 ± 0.5 Å (Fig. 4D). For the monophospho and dephospho lipid A variants the distance from the phosphate to the opposite hydroxyl group oxygen was considered instead. The *d*(P–P) decreased approximately to 11.7 ± 0.5 Å and 10.4 ± 0.2 Å, respectively for the synthetic analogues (Table 3). The solvent structure in the vicinity of the charged phosphates and polar hydroxyl groups was described by the RDF and CN curves computed for water oxygens (Fig. 4E,F, and Table 3). The RDF maximum for the first solvation shell was localised at a distance of R(P–w) = 3.7–3.8 Å for the phosphate groups and at R(O–w) = 2.9 Å for the C1- and C4′-hydroxyl groups. The average CN of 4.5–4.9 water molecules per phosphate group and 1.7–2.4 water molecules per C1- or C4′-hydroxyl group was determined for the first solvation shell (Table 3). The CNs of the C4′-phosphate or C4′-hydroxyl groups by water molecules were lower by 0.2 and 0.7, respectively compared to the same functional groups attached to the C1 carbon. This is most probably due to the steric repulsion effects of the neighbouring C6′-OH group.

In the simulation on LA-15-PP conducted in the presence of two Na^+ counterions the CNs of the phosphates fluctuated between 3.8–4.7 water molecules, which indicates high mobility of the counterions. RDF curves of the Na^+ ion distribution (Fig. 4G) showed two maxima at longer R(P–Na) distances of 6.8 and 8.2 Å with the net CNs of 0.2 and 0.6 for the C4′-phosphate group. A single maximum with the peak at 7.8 Å and coordination of 0.9 for the C1-phosphate group was found. Furthermore, the MRT curve for C4′-phosphate group coordination by Na^+ (Fig. 4H) revealed that the more distant second coordination shell is about two times more frequently populated than the first one, located closer to the phosphate oxygens. Animation of the MD trajectory, starting from the LA-15-PP structure with the sodium ions localised in the vicinity of the PO_4H^- groups, revealed that the two Na^+ ions were not constrained to the solvation shells of the phos-

phates but could travel across the solvent box. Comparison with the reports of Obst et al. [34] and Holst et al. [68] who predicted preferred positions of bivalent Ca^{2+} counterions in localised positions between two negatively charged carboxylic and phosphate groups of ReLPS showed the different behaviour of the monovalent Na^+ ions, which did not associate strongly with the phosphates.

The solute–solvent hydrogen bonding interactions and the bulk solvent effect of the surrounding water molecules stabilised the conformations of the charged and neutral lipid A analogues. A quantity proportional to solvation energy (E^{E}_{solv}) of the explicit solvation model was derived from the simulation trajectories in water (Table 3). The E^{E}_{solv} decreased with the decreasing formal charge of the lipid A analogues. For the LA-15-PP coordinated by Na^+ ions (LA-15-PP Na) it also included the contribution from averaged interaction with the Na^+ ions. By subtracting the E^{E}_{solv} value obtained for the LA-15-PP, computed without the presence of the counterions, the averaged interaction of the LA-15-PP analogue with the sodium counterions was estimated as $E_{ana} = -47$ kcal mol^{-1} per one PO_4H^-...Na^+ ion-pair. The instantaneous solute–solvent interactions of the lipid A analogues fluctuated by up to 20% around the mean value (Table 3 and Fig. 5). For comparison, we have computed E^{E}_{solv} of charged propylphosphate as a model of the phosphate group in lipid A, protonised propylamine and butane molecule using the explicit solvent model that included over 200 water molecules in the presence of Na^+ or Cl^- counterions. The derived E^{E}_{solv} magnitudes were equal to -114 kcal mol^{-1} for the propylamine, -131 kcal mol^{-1} for the propylphosphate, while the E^{E}_{solv} for the neutral butane molecule in water was equal to only -8 kcal mol^{-1}. The net interaction of propylamine and propylphosphate molecules with the Cl^- and Na^+ counterions rendered the interaction energies of -52 kcal mol^{-1} and -57 kcal mol^{-1}, respectively. These values corresponded roughly to the average energy of ion-pair formation of one phosphate group of lipid A with the Na^+ counterion in solution. The predicted explicit solvation energies of lipid A are comparable to the results obtained for larger molecules [65–67].

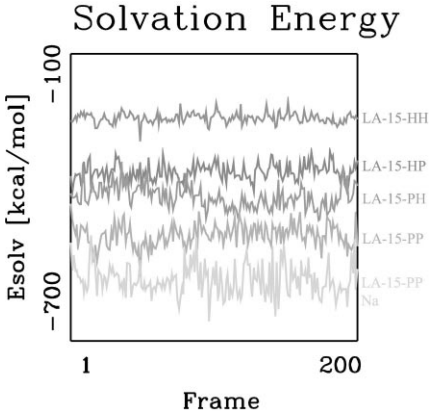

Fig. 5. Solvation energy of lipid A analogues. Explicit solvation energy E^{E}_{solv} of lipid A analogues computed each 0.5 ps during 100 ps MD simulation trajectory in a periodic solvent box with approximately 450 water molecules.

Solvation energies derived from the continuum PCM and DelPhi models yielded lower estimates for the energy of the solute–solvent interaction. These values correlated well with those derived from the explicit model (Table 3). Analysis of the

Table 4
Solvation of phosphate groups of lipid A from *E. coli* and its synthetic analogues

Property	LA-15-HH[a]	LA-15-HP	LA-15-PH	LA-15-PP
Q_{LA} [b]	0	−1	−1	−2
E^{P}_{solv} [c]	−119.3	−183.1	−210.2	−277.3
E^{P}_{solv} (P4′)[d]	−3.7	−6.9	−88.9	−104.5
E^{P}_{solv} (P1)	−4.3	−78.9	−6.8	−91.7
S_{vdw}(P4′)[e]	16.9	16.9	64.3	64.5
S_{vdw}(P1)	18.4	62.5	18.3	62.3

[a]For notation of lipid A analogues see Table 1.
[b]Molecular charge of the lipid A analogue (*e*).
[c]Solvation energy of lipid A analogues derived from the PCM continuum solvent model [58–60] (kcal mol^{-1}).
[d]Solvation energy contributions of the C4′–PO_4^-H (P4′) and C1–PO_4H^- (P1) groups derived from the PCM model (kcal mol^{-1}).
[e]van der Waals surface area of the C4′–PO_4H^- (P4′) and C1–PO_4H^- (P1) groups (Å^2).

relative contribution from the individual functional groups to the E^{P}_{solv} or E^{D}_{solv} in the bisphospho, monophospho and dephospho lipid A analogues confirmed the dominant role of phosphates in the interactions of lipid A moiety with polar environment. In the PCM continuum model the solvation of the phosphate groups contributed between 40 and 70% to total molecular solvation energy (Table 4). The interaction of the C4′–PO_4H^- group of LA-15-PH with the solvent was stronger than that of the C1–PO_4H^- group of LA-15-HP analogue. This can be attributed to steric and geometrical factors such as proximity of the C6′-hydroxymethyl group and solvent accessible surface area of the group. Different abilities of the C4′- and C1-phosphates to engage in polar interactions with the solvent may help to explain why the LA-15-PH and LA-15-HP analogues display different activities in the *Limulus* assay (Toxicolor test) [17].

3.4. Interactions of lipid A analogues with a receptor model

Interactions of the phosphate groups with water molecules or sodium counterions represent only a crude approximation of the specific lipid A-receptor interactions. MD simulations of lipid A analogues with their phosphate/hydroxyl groups bound to the HDM, a simple model of a receptor binding site with two charged ammonium groups that mimic the cationic side chains of lysine constrained to a certain distance and orientation, represent a more realistic description of the interactions of the lipid A moieties with protein receptor. The $-NH_3^+$ headgroups of HDM remained attached to the phosphate groups of LA-15-PP with a mean distance d(N–P) of 3.1 ± 0.1 Å during the whole simulation trajectory. The mean interaction energy of the LA-15-PP moiety with the HDM and the solvent molecules averaged over the trajectory amounted to $E^{E}_{int} = -561 \pm 24$ kcal mol^{-1} (Table 3). By subtracting the mean solvation energy of LA-15-PP obtained from the explicit solvent simulation (E^{E}_{solv}) the approximate interaction energy of LA-15-PP with the HDM receptor model was estimated as $E^{E}_{int} = -82$ kcal mol^{-1}. It corresponds roughly to a stabilisation energy of −41 kcal mol^{-1} per $PO_4H^-...NH_3^+$ ion-pair formation when we assume that the contribution of the aliphatic chain of HDM to the interaction with the lipid A was negligible compared with the energy of the ion-pair formation. Lower contributions from the C4′- or C1-hydroxyl groups of LA-15-PH, LA-15-HP and LA-15-HH to polar interactions with the ammonium groups of HDM significantly reduced the interaction energies to $E^{E}_{int} = -8$ kcal mol^{-1} per –OH group. The interaction energies of the bisphospho, monophospho and dephospho lipid A analogues with the HDM receptor model correlated well with the observed trend in experimental biological activities (Table 3):

LA-15-HH $|-16$ kcal mol$^{-1}|$

$<$LA-15-HP $|-46$ kcal mol$^{-1}|$

$<$LA-15-PH $|-52$ kcal mol$^{-1}|$

$<$LA-15-PP $|-82$ kcal mol$^{-1}|$

The more negative the interaction energy the higher is the predicted binding affinity of the lipid A analogue to the receptor model. The absolute values of E^{E}_{int} thus correlate with the trend of the increasing experimental activities [17].

In conclusion, the MD simulation on lipid A analogues and lipid A:receptor model complexes indicate that association of the lipid A moiety with polar molecules, measured by the solvation energies and lipid A-receptor interaction energies, is proportional to the number and position of the phosphate groups and correlates with the observed toxicity of the analogues [17].

3.5. Order and packing of fatty acid chains

Parallel alignment of the fatty acid chains of the starting structures was to a large extent preserved in all the lipid A analogues during the MD simulations in solution. A tilt angle between the disaccharide headgroup axis and the mean longitudinal direction of the fatty acid chains was found to vary between 69 and 96° (Table 3). The apparent length L_{aver} of the acyl chains remained in the range of 12.1–12.9 Å for all six chains in all the considered analogues. For comparison, the length of an equivalent $C_{12}H_{26}$ hydrocarbon chain in the all-*trans* conformation d(C_1–C_{12}) is equal to 13.8 Å. The order parameter for acyl

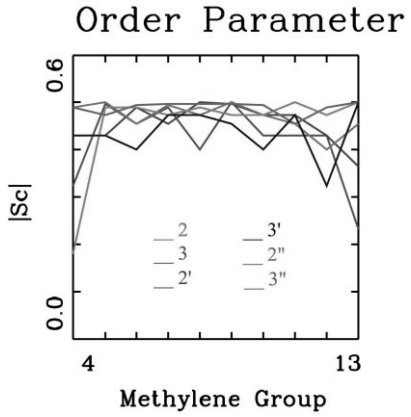

Fig. 6. Profiles of order parameter of fatty acid chains. $|S_c|$ for six chains of solvated lipid A analogue LA-15-PP coordinated by two Na^+ ions averaged over 100 ps MD simulation trajectory.

chains $|S_c|$, depicted for the last 10 methylene groups of the six {2,3,2′,2″,3′,3″} fatty acid chains of LA-15-PP (Fig. 6), was calculated from the magnitudes of $\langle\cos^2\theta\rangle$ averaged over the MD trajectory. The value of the order parameter started at lower magnitude at the first considered methylene group of the chain end linked to the headgroup (C4), $|S_c|$ then increased up to 0.5 towards the middle of the chain and decreased again towards the free chain end (C13) (Fig. 6). This pattern was, however, not common to all the acyl chains. The {2′,2″,3′,3″} acyl chains showed somewhat lower tendency for disordered chain ends than the {2,3} chains, probably due to closer contacts and attractions from the neighbouring chains. A similar order pattern for fatty acid chains of ReLPS was also observed by Obst et al. [34]. Model calculations for aggregated phospholipids by Israelachvili et al. [63] predicted that the order parameter remained constant along the chain and dropped only near the chain end. A possible explanation for the lower $|S_c|$ values of methylene groups near the GlcN-II-GlcN-I headgroup is that they are fixed in specific orientations by the amide-/ester-linkages [34]. In general we can conclude that the fatty acid chains spent most of the MD simulation time in water in a nearly extended conformation and retained an ordered compact parallel alignment.

The packing parameter of the lipid A analogues was estimated for the averaged structures obtained by averaging over the recorded MD configurations and a subsequent stereochemical refinement. The approximate cross-section of the GlcN-II-GlcN-I headgroup was estimated between 86 $Å^2$ and 142 $Å^2$ for the four analogues and depended on the number of the phosphate groups in the molecule and presence of the Na^+ counterions (Table 3). The resulting packing parameter P was found within interval 0.9–1.5. Our estimate of the packing parameter suggests that the LA-15-PP analogue prefers lamellar aggregates ($P<1$) while the remaining three monophospho and dephospho lipid A analogues show a preference for non-lamellar aggregates ($P>1$).

The supramolecular structure of different lipid A and LPS forms has been studied in the past and led to the conclusion that the endotoxic potency of a lipid A sample may be related to the ability to adopt non-lamellar structures [4]. In the series of the four considered lipid A analogues the biological activity parameter [17] is roughly proportional to the number and position of the phosphate groups in the molecular structure and increases with the increasing number of phosphates. On the other hand, the predicted tendency to form non-lamellar aggregates, under the conditions of the present study was found to increase with the decreasing number of phosphate groups, which contradicts the conclusions of Brandenburg et al. [4]. Recent reports have shown that specific interactions with cell surface receptors are probably responsible for the biological effects rather than the non-specific effect of the supramolecular structure of the lipid A or LPS aggregates [9–14].

4. Conclusions

The present study has demonstrated that even though the chemical structures of the lipid A analogues are different, these molecules share common conformational and dynamic features such as the molecular shape, disaccharide headgroup conformation, phosphate group orientation, compact aligned packing and order of the fatty acid chains, tilt and bend angles of the headgroup and the hydrophobic chains. The bisphospho, monophospho and dephospho lipid A analogues differ in the number and position of the attached phosphate groups and the resulting physicochemical properties such as molecular charge, solvation energy, reactivity towards charged

and polar species and ability to form ion-pairs and hydrogen bonds with polar or cationic proton donors. Experimental data on biological activity of the lipid A analogues [17] showed that the activities increase with the number of phosphate groups in the lipid A moiety and depend on the position of the phosphate groups in the GlcN-II and GlcN-I rings. Explanation of the observed relationship between the chemical structure and biological potency was derived from simple mechanistic models.

The capability of lipid A variants to adopt non-lamellar structures, which is dependent on the molecular shape (and is related to the ability of the fatty acid chains to intercalate into the phospholipid membrane of a host cell) has been suggested to be related to their bioactivities [4]. The molecular packing parameter of solvated lipid A analogues and the ability to form non-lamellar aggregates predicted from MD simulations according to Israelachvili [63] did not correlate with the experimental biological activities. On the other hand, we have shown that the biological activity data of the four analogues correlated well with those physicochemical properties that determine interactions of the phosphate groups with polar solvents or charged proton donor groups of a hypothetical receptor binding site. The ability of the phosphate groups to engage in hydrogen bonding and ion-pair formation were described by the solvation energy, RDF, CN and interaction energies of the lipid A analogues to the HDM model receptor. Thus a molecular mechanism of lipid A action that assumes polar interactions of the phosphates with a receptor binding site, which contains two cationic amino acid residues (such as lysine) in a suitable geometrical arrangement to complement the lipid A headgroup, can rationalise the observed trend in biological activities of the lipid A analogues. Interaction energy of lipid A analogues to the model receptor is proportional to the number as well as position of the phosphate groups in the lipid A moiety and correlates with the experimental bioactivities of the analogues. Thus a mechanism of action that assumes specific ion-pair formation between the phosphates and the cationic amino acids of the receptor model rationalises the observed structure–activity relationships. Presence of cationic side chains at the receptor binding sites has been repeatedly reported in LPS-binding sequences of peptides and proteins, which are rich in basic amino acid residues and display an amphipathic character [20–26]. Therefore, a mechanism of action that involves interactions of the charged phosphate groups seems to be more plausible than an alternative mechanism, which assumes the molecular shape, aggregation and interactions of the fatty acid chains with the host cell membrane.

Details of construction of a more realistic peptidic pseudoreceptor model and description of lipid A binding to amino acid sequences of the amphipathic binding site are elaborated in a parallel study [69].

Some cationic amphipathic drugs and peptides have been reported to interact with the lipid A while the resulting complexes are virtually inactive [23,26,70]. Therefore, a possible therapeutic approach aimed at neutralisation of biological effects of lipid A could be based on the design of cationic amphipathic peptides or drugs with a complementary structure to the lipid A headgroup that would form ion-pairs with the phosphates and thus compete with the host cell receptors for lipid A binding.

Acknowledgements

This work was supported by the National Science and Technology Board (NSTB Grant No. 17/4/19). V.F. is on leave from Cancer Research Institute, Slovak Academy of Sciences, 83391 Bratislava, Slovakia.

References

[1] E.Th. Rietschel, H. Brade, O. Holst, L. Brade, S. Müller-Loennies, U. Mamat, U. Zähringer, F. Beckmann, U. Seydel, K. Brandenburg, A.J. Ulmer, T. Mattern, H. Heine, S. Schletter, S. Hauschildt, H. Loppnow, U. Schönbeck, H.-D. Flad, U.F. Schade, F. DiPadova, S. Kusumoto, R.R. Schumann, Bacterial endotoxin: chemical constitution, biological recognition, host response, and immunological detoxification, Curr. Top. Microbiol. Immunol. 216 (1995) 39–81.

[2] H. Takada, S. Kotani, Structural requirements of lipid A for endotoxic and other biological activities, CRC Crit. Rev. Microbiol. 16 (1989) 477–523.

[3] S.M. Opal, R.J. Yu Jr., Anti-endotoxin strategies for the prevention and treatment of septic shock. New approaches and future directions, Drugs 55 (1998) 497–508.

[4] K. Brandenburg, H. Mayer, M.J. Koch, J. Weckesser, E.Th. Rietschel, U. Seydel, Influence of the supramolecular struc-

ture of free lipid A on its biological activity, Eur. J. Biochem. 218 (1993) 555–563.
[5] S. Iwanaga, T. Morita, T. Miyata, T. Nakamura, Hemolymph coagulation system in *Limulus*, in: L. Schlessinger (Ed.), Microbiology, American Society for Microbiology, Washington D.C., 1985, pp. 29–32.
[6] I. Mattsby-Baltzer, K. Lindgren, B. Lindholm, L. Edebo, Endotoxin shedding by enterobacteria: free and cell-bound endotoxin differ in *Limulus* activity, Infect. Immun. 59 (1991) 689–695.
[7] K. Takayama, D.H. Mitchel, Z.Z. Din, P. Mukerjee, C. Li, D.L. Coleman, Monomeric Re lipopolysaccharide from *Escherichia coli* is more active than aggregated form in the *Limulus* amoebocyte lysate assay and in inducing Egr-1 mRNA in murine macrophages, J. Biol. Chem. 269 (1994) 2241–2244.
[8] S. Kotani, H. Takada, M. Tsujimoto, T. Ogawa, I. Takahashi, T. Ikeda, K. Otsuka, H. Shimauchi, N. Kasai, J. Mashimo, S. Nagao, A. Tanaka, S. Tanaka, K. Harada, K. Nagaki, H. Kitamura, T. Shiba, S. Kusumoto, M. Imoto, H. Yoshimura, Synthetic lipid A with endotoxic and related biological activities comparable to those of a natural lipid A from an *Escherichia coli* RE-mutant, Infect. Immun. 49 (1985) 225–237.
[9] Ch.R.H. Raetz, Bacterial endotoxins: extraordinary lipids that activate eucaryotic signal transduction, J. Bacteriol. 175 (1993) 5745–5753.
[10] R.J. Ulevich, P.S. Tobias, Recognition of Gram-negative bacteria and endotoxin by the innate immune system, Curr. Opinion Immunol. 11 (1999) 19–22.
[11] R.R. Schumann, S.R. Leong, G.W. Flags, P.W. Gray, S.D. Wright, J.C. Mathison, P.S. Tobias, R.J. Ulevich, Structure and function of lipopolysaccharide binding protein, Science 249 (1990) 1429–1431.
[12] S.D. Wright, R.A. Ramos, P.S. Tobias, R.J. Ulevich, J.C. Mathinson, CD14, a receptor for complexes of lipopolysaccharide (LPS) and LPS binding protein, Science 249 (1990) 1431–1433.
[13] R.B. Yang, M.R. Mark, A. Gray, A. Huang, M.H. Xie, H. Zhang, A. Goddard, W.I. Wood, A.L. Gurney, P.J. Godowski, Toll-like receptor-2 mediates lipopolysaccharide-induced cellular signalling, Nature 17 (1998) 284–288.
[14] F.L. Rock, G. Hardiman, J.C. Timas, R.A. Kastelein, J.F. Bazan, A family of human receptors structurally related to *Drosophila* toll, Proc. Natl. Acad. Sci. USA 95 (1998) 588–593.
[15] O. Lüderitz, C. Galanos, V. Lehmann, H. Meyer, E.Th. Rietschel, J. Weckesser, Chemical structure and biological activities of lipid A's from various bacterial families, Naturwissenschaften 65 (1978) 578–585.
[16] M. Mayer, J.H. Krauss, A. Yokota, J. Weckesser, Natural variants of lipid A, in: H. Friedman, T.W. Klein, M. Nakano, A. Nowotny (Eds.), Endotoxin, Plenum Press, New York, 1990, pp. 45–70.
[17] H. Takada, S. Kotani, S. Tanaka, T. Ogawa, I. Takahashi, M. Tsujimoto, T. Kumuro, T. Shiba, S. Kusumoto, N. Kusunose, A. Hasegawa, M. Kiso, Structural requirements of lipid A species in activation of clotting enzymes from the horseshoe crab, and the human complement cascade, Eur. J. Biochem. 175 (1988) 573–580.
[18] T. Kirikae, F.U. Schade, U. Zähringer, F. Kirikae, H. Brade, S. Kusumoto, T. Kusama, E.Th. Rietschel, The significance of the hydrophilic backbone and the hydrophobic fatty acid regions of lipid A for macrophage binding and cytokine induction, FEMS Immun. Med. Microbiol. 8 (1994) 13–26.
[19] A.B. Schromm, K. Brandenburg, H. Loppnow, U. Zähringer, E.Th. Rietschel, S.F. Carroll, M.H.J. Koch, S. Kusumoto, U. Seydel, The charge of endotoxin molecules influences their conformation and IL-6-inducing capacity, J. Immunol. 161 (1998) 5464–5471.
[20] P.S. Tobias, K. Soldau, R.J. Ulevitch, Identification of a lipid A binding site in the acute phase reactant lipopolysaccharide binding protein, J. Biol. Chem. 264 (1989) 10867–10871.
[21] A. Hoess, S. Watson, G.R. Siber, R. Liddington, Crystal structure of an endotoxin-neutralising protein from the horseshoe crab, *Limulus* anti-LPS factor, at 1.5 Å resolution, EMBO J. 12 (1993) 3351–3356.
[22] L.J. Beamer, S.F. Carroll, D. Eisenberg, Crystal structure of human BPI and two bound phospholipids at 2.4 Å resolution, Science 276 (1997) 1861–1864.
[23] A. Rustici, M. Velucchi, R. Faggioni, M. Sironi, P. Ghezzi, S. Quataet, B. Green, M. Porro, Molecular mapping and detoxification of the lipid A binding site by synthetic peptides, Science 259 (1993) 361–365.
[24] H.A. Pereira, I. Erdem, J. Pohl, J.K. Spitznagel, Synthetic bactericidal peptide based on CAP37: a 37-kDa human neutrophil granule-associated cationic antimicrobial protein chemotactic for monocytes, Proc. Natl. Acad. Sci. USA 90 (1993) 4733–4737.
[25] E. Elass-Rochard, A. Roseanu, D. Legrand, M. Trif, V. Salmon, C. Motas, J. Montreuil, G. Spik, Lactoferrin–lipopolysaccharide interaction: involvement of the 28–34 loop region of human lactoferrin in the high affinity binding to *Escherichia coli* O55B5 lipopolysaccharide, Biochem. J. 312 (1995) 839–845.
[26] G.-H. Zhang, D.M. Mann, C.-M. Tsai, Neutralisation of endotoxin in vitro and in vivo by human lactoferrin-derived peptide, Infect. Immun. 67 (1999) 1353–1358.
[27] P.A. Kollman, Advances and continuing challenges in achieving realistic and predictive simulations of the properties of organic and biological molecules, Acc. Chem. Res. 29 (1996) 461–469.
[28] T.J. Marrone, J.M. Briggs, J.A. McCammon, Structure-based drug design: computational advances, Annu. Rev. Pharmacol. Toxicol. 37 (1997) 71–90.
[29] M. Kastowsky, A. Sabisch, T. Gutberlet, H. Bradaczek, Molecular modelling of bacterial deep rough mutant lipopolysaccharide of *Escherichia coli*, Eur. J. Biochem. 197 (1991) 707–716.
[30] M. Kastowsky, T. Gutberlet, H. Bradaczek, Molecular mod-

elling of three-dimensional structure and conformational flexibility of bacterial lipopolysaccharide, J. Bacteriol. 174 (1992) 4798–4806.
[31] Y. Wang, R.I. Hollingsworth, An NMR and molecular mechanics study of the molecular basis for the supramolecular structure of lipopolysaccharides, Biochemistry 35 (1996) 5647–5654.
[32] S. Jung, D. Min, R.I. Hollingsworth, A Metropolis Monte Carlo method for analyzing the energetics and dynamics of lipopolysaccharide supramolecular structure and organization, J. Comput. Chem. 17 (1996) 238–249.
[33] E.V. Vinogradov, R. Stuike-Prill, K. Bock, O. Holst, H. Brade, The structure of the carbohydrate backbone of the core-lipid-A region of the lipopolysaccharide from *Vibrio cholerae* strain H11 (non-O1), Eur. J. Biochem. 218 (1993) 543–554.
[34] S. Obst, M. Kastowsky, H. Bradaczek, Molecular dynamics simulations of six different fully hydrated monomeric conformers of *Escherichia coli* Re-lipopolysaccharide in the presence and absence of Ca^{2+}, Biophys. J. 72 (1997) 1031–1046.
[35] A.D. Ferguson, E. Hofman, J.W. Coulton, K. Diederichs, W. Welte, The crystal structure of ferric hydroxamate receptor (Fhua) from *E. coli* with bound lipopolysaccharide: structural basis for siderophore mediated iron transport, PDB entry 1FCP, to be published.
[36] Insight II®, Discover®, DelPhi and Biopolymer User Guide, Biosym/MSI, October 1995, San Diego, CA.
[37] J.R. Maple, U. Dinur, A.T. Hagler, Derivation of forcefields for molecular mechanics and dynamics from ab initio energy surfaces, Proc. Natl. Acad. Sci. USA 85 (1988) 5350–5354.
[38] J.R. Maple, M.-J. Hwang, T.P. Stockfish, U. Dinur, M. Waldman, C.S. Ewing, A.T. Hagler, Derivation of class II force fields. 1. Methodology and quantum force filed for the alkyl functional group and alkane molecules, J. Comput. Chem. 15 (1994) 162–182.
[39] J.M. Asensio, M. Martin-Pastor, J. Jimenez-Barbero, The use of CVFF and CFF91 force fields in conformational analysis of carbohydrate molecules. Comparison with AMBER molecular mechanics and dynamics calculations for methyl α-lactoside, Int. J. Biol. Macromol. 17 (1995) 137–148.
[40] M. Martin-Pastor, J.F. Espinosa, J.M. Asensio, J. Jimenez-Barbero, A comparison of the geometry and of the energy results obtained by the application of different molecular mechanics forcefields to methyl α-lactoside and the C-analogue of lactose, Carbohydr. Res. 298 (1997) 15–49.
[41] J. Perlstein, K. Steppe, S. Vaday, E.M.N. Ndip, Molecular self-assemblies. 5. Analysis of the vector properties of hydrogen bonding in crystal engineering, J. Am. Chem. Soc. 118 (1996) 8433–8443.
[42] K. Gundertofte, T. Liljefors, P.O. Norrby, A comparison of conformational energies calculated by several molecular mechanics methods, J. Comput. Chem. 17 (1996) 429–449.
[43] D.A. Cumming, J.P. Carver, Virtual and solution conformations of oligosaccharides, Biochemistry 26 (1987) 6664–6676.
[44] M.K. Dowd, A.D. French, P.J. Reilly, Conformational analysis of the anomeric forms of sophorose, laminarabiose, and cellobiose using MM3, Carbohydr. Res. 233 (1992) 15–34.
[45] M.P. Allen, D.J. Tildesley, Computer Simulations of Liquids, Oxford University Press, Oxford, 1987.
[46] D.A. Brant, Shapes and motions of polysaccharide chains, Pure Appl. Chem. 69 (1997) 1885–1892.
[47] R.J. Woods, Computational carbohydrate chemistry: what theoretical methods can tell us, Glycoconjugate J. 15 (1998) 209–216.
[48] B.J. Hardy, The glycosidic linkage flexibility and time-scale similarity hypotheses, J. Mol. Struct. (Theochem) 395–396 (1997) 187–200.
[49] A.C. Bush, M. Martín-Pastor, Structure and conformation of complex carbohydrates of glycoproteins, glycolipids, and bacterial polysaccharides, Annu. Rev. Biophys. Biomol. Struct. 28 (1999) 269–293.
[50] S. Doniach, P. Eastman, Protein dynamics simulations from nanoseconds to microseconds, Curr. Opin. Struct. Biol. 9 (1999) 157–163.
[51] A. Poveda, J.L. Asensio, M. Martín-Pastor, M. Jiménez-Barbero, Solution conformation and dynamics of a tetrasaccharide related to the $Lewis^X$ antigen deduced by NMR relaxation measurements, J. Biomol. NMR 10 (1997) 29–43.
[52] S.B. Engelsen, S. Perez, Internal motions and hydration of sucrose in a dilute water solution, J. Mol. Graph. Model. 15 (1997) 122–131.
[53] Q. Liu, R.K. Schmidt, B. Teo, P.A. Karplus, J.W. Brady, Molecular dynamics studies of the hydration of α,α-trehalose, J. Am. Chem. Soc. 119 (1997) 7851–7862.
[54] L. Mãler, G. Widmaln, J. Kowalewski, Motional properties of a pentasaccharide containing a 2, 6-branched manose residue as studied by ^{13}C nuclear spin relaxation, J. Biomol. NMR 7 (1996) 1–7.
[55] J.R. Brisson, S. Uhrinova, R.J. Woods, M. van der Zwan, H.C. Jarrell, L.C. Paoletti, D.L. Kasper, H.J. Jennings, NMR and molecular dynamics studies of the conformational epitope of the type III group B *Streptococcus* capsular polysaccharides and derivatives, Biochemistry 36 (1997) 3278–3292.
[56] A.E. Garcia, L. Stiller, Computation of the mean residence time of water in the hydration shells of biomolecules, J. Comput. Chem. 14 (1993) 1396–1406.
[57] V. Frecer, S. Miertus, A. Tossi, D. Romeo, Rational design of inhibitors for drug-resistant HIV-1 aspartic protease mutants, Drug Des. Discov. 15 (1998) 211–231.
[58] J. Tomasi, M. Persico, Molecular interactions in solutions: An overview of methods based on continuous distributions of the solvent, Chem. Rev. 94 (1994) 2027–2094.
[59] S. Miertus, E. Scrocco, J. Tomasi, Electrostatic interaction of a solute with a continuum. A direct utilization of ab initio molecular potentials for the prevision of solvent effect, Chem. Phys. 55 (1981) 117–129.
[60] V. Frecer, S. Miertus, Polarizable continuum model of solvation for biopolymers, Int. J. Quantative Chem. 42 (1992) 1449–1468.

[61] B.T. Thole, Molecular polarizabilities calculated with a modified dipole interaction, Chem. Phys. 59 (1981) 341–350.
[62] J. Seelig, A. Seelig, The dynamic structure of fatty acyl chains in a phospholipid bilayer measured be deuterium magnetic resonance, Biochemistry 13 (1974) 4839–4845.
[63] J.N. Israelachvili, Intermolecular and Surface Forces, Academic Press, London, 1991.
[64] C. Tanford, Micelle shape and size, J. Phys. Chem. 76 (1972) 30203–30224.
[65] C.L. Brooks, M. Karplus, Solvent effect on protein motions and protein effect on solvent motions. Dynamics of the active site region of lysozyme, J. Mol. Biol. 208 (1989) 159–181.
[66] P.J. Steinbach, B.R. Brooks, Protein hydration elucidated by molecular dynamics simulations, Proc. Natl. Acad. Sci. USA 90 (1993) 9135–9139.
[67] W.F. van Gunsteren, F.J. Luque, D. Timms, A.E. Torda, Molecular mechanics in biology: from structure to function, taking account of solvation, Annu. Rev. Biophys. Biomol. Struct. 23 (1994) 847–863.
[68] O. Holst, W. Broer, J.E. Thomas-Oates, U. Mamat, H. Brade, Structural analysis of two oligosaccharide bisphosphates from the lipopolysaccharide of a recombinant strain of *Escherichia coli* F515 (Re chemotype) expressing the genus-specific epitope of *Chlamydia* lipopolysaccharide, Eur. J. Biochem. 214 (1993) 703–710.
[69] V. Frecer, B. Ho, J.L. Ding, Interpretation of biological activity data of bacterial endotoxins by simple molecular models of mechanism of action, Eur. J. Biochem. 267 (2000) 837–852.
[70] S.A. David, B. Bechtel, C. Annaiah, V.I. Mathan, P. Balaram, Interaction of cationic amphiphilic drugs with lipid A: implications for development of endotoxemia antagonists, Biochim. Biophys. Acta 1212 (1994) 167–175.